

Heterogeneous & Homogeneous & Bio- & Nano-

# CHEMCATCHEM

CATALYSIS

## Accepted Article

**Title:** Direct Synthesis of Ultra-small Ruthenium Nanoparticles on Porous Supports Using Natural Sources for Highly Efficient and Selective Furfural Hydrogenation

**Authors:** Zhanrong Zhang, Jinliang Song, Zhiwei Jiang, Qinglei Meng, Pei Zhang, and Buxing Han

This manuscript has been accepted after peer review and appears as an Accepted Article online prior to editing, proofing, and formal publication of the final Version of Record (VoR). This work is currently citable by using the Digital Object Identifier (DOI) given below. The VoR will be published online in Early View as soon as possible and may be different to this Accepted Article as a result of editing. Readers should obtain the VoR from the journal website shown below when it is published to ensure accuracy of information. The authors are responsible for the content of this Accepted Article.

**To be cited as:** *ChemCatChem* 10.1002/cctc.201700262

**Link to VoR:** <http://dx.doi.org/10.1002/cctc.201700262>

# Direct Synthesis of Ultra-small Ruthenium Nanoparticles on Porous Supports Using Natural Sources for Highly Efficient and Selective Furfural Hydrogenation

Zhanrong Zhang<sup>[a]</sup>, Jinliang Song<sup>\*[a]</sup>, Zhiwei Jiang<sup>[a]</sup>, Qinglei Meng<sup>[a]</sup>, Pei Zhang<sup>[a]</sup> and Buxing Han<sup>\*[a, b]</sup>

**Abstract:** Synthesis of noble metal nanoparticles (NPs) with ultra-small particle sizes (< 2nm) is crucially important, but challenging. Making use of the unique structure of natural sources for the preparation of functional materials is an attractive topic. Taking advantage of the coordination effect between polyphenols and metal ions, we report a straightforward strategy for the synthesis of porous heterogeneous catalysts containing ultra-small Ru NPs. These catalysts exhibited excellent catalytic activity for selective hydrogenation of furfural. We envisage this strategy would find a broad range of applications in the near future.

Heterogeneous catalysis plays a key role for the enhancement of the efficiency of many chemical reactions. It represents one of the most important and widely applied chemical processes of various industries. Many heterogeneous catalysts involve noble metal nanoparticles (NPs) which provide the active sites and a support on which the NPs are dispersed. Numerous studies have verified that the sizes and structures of metal NPs significantly affect their catalytic performances.<sup>1</sup> Reductions in the sizes of noble metal NPs afford higher surface to volume ratio and larger proportion of surface atoms, resulting in predominantly edge and corner atoms.<sup>2</sup> To this end, the design and synthesis of supported ultra-small noble metal NPs (particle diameter < 2 nm) is gaining increasingly substantial attention.<sup>3,4</sup>

However, at nano size regime, metal NPs are unstable and tend to aggregate, owing to their high surface energy and surface to volume ratio.<sup>5</sup> Also, the low affinity between metal precursors or nano catalysts and their supports generally leads to NPs with large particle sizes ranging from several nanometers to micrometers. This renders the conventional fabrication protocols (e.g., coprecipitation, impregnation) impractical and ineffective for rational control of particle sizes and dispersion.<sup>3</sup> Noble metal NPs with controlled particle sizes and nanostructures could be produced with the aid of capping agents. However, in this case, the presence of capping agents might render the catalysts less effective and/or selective by blocking the active sites.<sup>3</sup> Despite these capping agents could be removed by thermal decomposition, the small metal NPs tend to sinter and/or aggregate to form larger particles.<sup>6</sup> In another aspect, introduction of porosity to heterogeneous catalysts affects the diffusion of reactants and product distribution, and could generally enhance the catalytic efficiency.<sup>5,7</sup> Hence, the development of general and readily applicable methodologies for

the fabrication of ultra-small noble metal NPs supported on porous supports is highly desirable, but represents a grand challenge, from both fundamental and practical point of view.

In recent years, innovative design and synthesis of functional materials using natural resources derived compounds is gaining significant attention.<sup>8</sup> Owing to the diverse and unique structures and properties of some naturally occurring components, a wide array of functional materials could be produced with many different applications. For example, polyphenols are a group of compounds which are widely distributed in plant tissues and display a diverse spectrum of chemical and physical properties.<sup>9,10</sup> Due to their high dihydroxyphenyl (catechol) and trihydroxyphenyl (gallic acid) content, some polyphenols could chelate with metal ions to generate many functional materials. These materials have found a diverse range of applications such as cell encapsulation,<sup>11</sup> catalysis,<sup>12,13</sup> multifunctional coatings,<sup>14</sup> and capsules.<sup>15</sup>

Inspired by the coordination effect between polyphenol molecules and metal ions as well as the abovementioned applications, we anticipate that the polyphenol-metal complexes could also be used as ideal precursors for the synthesis of ultra-small metal NPs. Herein, we report a novel and straightforward strategy for synthesis of ultra-small Ru NPs that are uniformly dispersed on supports with mesoporosity, taking advantage of the coordination effect between natural resource derived tannic acid (TA), Ru<sup>3+</sup> and Ti<sup>4+</sup>.

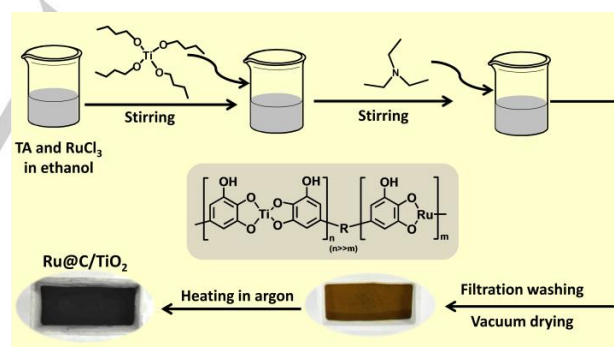


**Figure 1.** Illustration for the synthesis of Ru@C/TiO<sub>2</sub> catalysts.

Figure 1 highlights our procedure for the preparation of mesoporous catalysts containing ultra-small Ru NPs using TA, tetrabutyl titanate and RuCl<sub>3</sub>·3H<sub>2</sub>O as precursors. TA is a low-cost, abundant and naturally occurring polyphenol and has a high dihydroxyphenyl content (Figure S1 and S2). The abundant dihydroxyphenyl groups in TA could chelate with metal ions. Hence, the Ru ions could be captured or “grasped” by the OH groups while stirring in ethanol solution at room temperature. Subsequently, tetrabutyl titanate was added dropwise into the mixture and the Ti ions coordinate with the abundant dihydroxyphenyl groups. The insert in Figure 1 highlights a proposed possible schematic structure illustrating the coordination effect between TA, Ru<sup>3+</sup> and Ti<sup>4+</sup>. This structure

[a] Dr. Z. Zhang, Dr. J. Song, Dr. Z. Jiang, Dr. Q. Meng, Dr. P. Zhang, Prof. B. Han

Beijing National Laboratory for Molecular Sciences, Key Laboratory of Colloid and Interface and Thermodynamics, Institute of Chemistry, Chinese Academy of Sciences, Beijing 100190, P. R. China

[b] University of Chinese Academy of Sciences, Beijing 100049, P. R. China

E-mail: songjl@iccas.ac.cn, hanbx@iccas.ac.cn

Supporting information for this article is given via a link at the end of the document.

was speculated according to Wei et al. In their recent work, they have proposed similar structures demonstrating the self-assembled Fe-TA<sup>12a</sup> and Co-TA<sup>12b</sup> framework. Due to this coordination effect, brown precipitates were formed while stirring. Followed by deprotonation with triethylamine, these precipitates were washed with ethanol, vacuum dried, grinded before heating at elevated temperatures (400 °C, 500 °C, 600 °C and 700 °C) under argon atmosphere to afford Ru@C/TiO<sub>2</sub> catalysts.

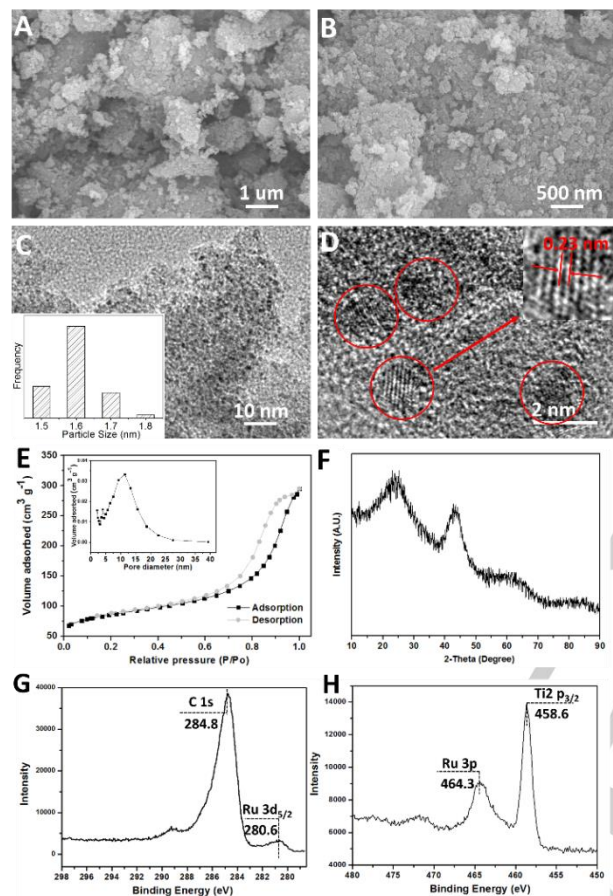


**Figure 2.** Characterization of the Ru@C/TiO<sub>2</sub>-500. (A, B) SEM images, (C) TEM image, the insert is particle size distribution histogram of the Ru NPs (Data was obtained from about 200 Ru particles). (D) HRTEM image, the Ru NPs are highlighted by the red circles, (E) N<sub>2</sub> adsorption-desorption isotherm, the insert is pore size distribution, (F) powder XRD pattern, and (G, H) XPS spectra.

The synthesized Ru@C/TiO<sub>2</sub> catalysts were characterized by a variety of analytical techniques including scanning electron microscopy (SEM), transmission electron microscopy (TEM), high-resolution TEM (HRTEM), X-ray diffraction (XRD), X-ray photoelectron spectroscopy (XPS) and N<sub>2</sub> adsorption-desorption method. SEM examinations (Figure 2A and 2B) revealed that the sample heated at 500 °C (denoted as Ru@C/TiO<sub>2</sub>-500) possesses an ununiform shape. The Ru NPs are uniformly dispersed and the average diameter of these NPs is around 1.6 ± 0.12 nm with a narrow size distribution, as shown in the TEM image of this sample (Figure 2C and the insert illustrating the histogram of Ru particle size distribution). From the high-resolution TEM (HRTEM) image (Figure 2D), the Ru NPs could

be clearly observed and highlighted by the red circles. The interplanar distance of the Ru NPs for the lattice fringe was around 0.23 nm, which is the distinct lattice fringe of Ru crystal. The small particle size and narrow size distribution was resulted from the coordination effect between Ru ions and dihydroxyphenyl groups of TA. The N<sub>2</sub> adsorption-desorption method indicates that the Ru@C/TiO<sub>2</sub>-500 was also porous with mesopores centered at around 8.8 nm. The surface area and pore volume was around 293 m<sup>2</sup> g<sup>-1</sup> and 0.39 cm<sup>3</sup> g<sup>-1</sup>, respectively (Figure 2E). The loading amount of Ru NPs in Ru@C/TiO<sub>2</sub>-500 was around 1.16%, as determined by the ICP-AES analysis (Table S1). The XRD pattern of Ru@C/TiO<sub>2</sub>-500 (Figure 2F) suggests that this material has low crystallinity or is poorly ordered, indicating that the structure of this material is nearly amorphous. Meanwhile, no obvious Ru bands exist in the XRD pattern of Ru@C/TiO<sub>2</sub>-500, resulting from the well dispersion of Ru with ultrafine particles.<sup>16</sup> The X-ray photoelectron spectrum (XPS) showed peaks of Ru 3p<sub>3/2</sub> and 3d<sub>5/2</sub> at the binding energies of 464.3 eV and 280.6 eV, respectively, corresponding to Ru 3p<sub>3/2</sub> and Ru 3d<sub>5/2</sub> of Ru(0), which further confirmed the generation of Ru NPs. Additionally, control experiments indicated that the materials prepared without using TA or tetrabutyl titanate was non-porous with very low surface area and the Ru NPs in these two materials were aggregated seriously. These results confirmed the significant effect of TA and tetrabutyl titanate as discussed above in the preparation of this supported ultra-small Ru NPs on porous C/TiO<sub>2</sub>.

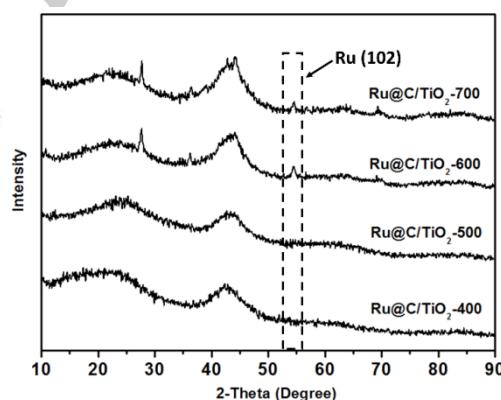


**Figure 3.** Powder XRD pattern of Ru@C/TiO<sub>2</sub> catalysts.

We also synthesized Ru@C/TiO<sub>2</sub> by heating at various temperatures (400 °C, 600 °C and 700 °C) and the samples are denoted as Ru@C/TiO<sub>2</sub>-400, Ru@C/TiO<sub>2</sub>-600 and Ru@C/TiO<sub>2</sub>-700 accordingly. The Ru@C/TiO<sub>2</sub>-400 has very similar textural and structural properties to Ru@C/TiO<sub>2</sub>-500 (Table S2, Figure S3 and S6). From Table S2, the pore diameter of the prepared catalysts at different calcination temperature changed from 7.4 nm to 15.3 nm, while the surface area showed no such obvious difference. It is known that at higher calcination temperature, more organic components were decomposed and more gases were released, resulting in more micropores. Hence, the surface area could be potentially increased.<sup>17a</sup> However, higher calcination temperature could result in the impenetration of

mesopores in the meantime, which caused the decrease of the surface area.<sup>17b</sup> Hence, it is possible that the difference between the surface areas of the prepared catalysts is not very significant due to the abovementioned two opposite effects. Moreover, the Ru NPs contained in Ru@C/TiO<sub>2</sub>-600 and Ru@C/TiO<sub>2</sub>-700 featured large particle sizes with slightly wider size distribution, as Ru NPs inevitably agglomerated at elevated temperatures (Figure S4 and S5). This is also reflected in the XRD patterns of Ru@C/TiO<sub>2</sub>-600 and Ru@C/TiO<sub>2</sub>-700 (Figure 3). Characteristic band of Ru(0) at about 2 $\theta$ =54° ascribing to Ru(102) could be observed in the XRD patterns of Ru@C/TiO<sub>2</sub>-600 and Ru@C/TiO<sub>2</sub>-700, but not in those of Ru@C/TiO<sub>2</sub>-400 and Ru@C/TiO<sub>2</sub>-500.<sup>18</sup> This effect is primarily due to the larger particle sizes of Ru NPs contained in the former two samples. XPS analysis confirms the presence of Ru(0) NPs in Ru@C/TiO<sub>2</sub>-400, Ru@C/TiO<sub>2</sub>-600 and Ru@C/TiO<sub>2</sub>-700 (Figure S7 and S8). It is also noteworthy that the Ru@C/TiO<sub>2</sub>-600 and Ru@C/TiO<sub>2</sub>-700 are also mesoporous while the pore sizes are larger than those of Ru@C/TiO<sub>2</sub>-400 and Ru@C/TiO<sub>2</sub>-500, as more organic matter was decomposed when treated at higher temperatures (Figure S6, Table S2). This effect also leads to the decreased amount of the obtained support (C/TiO<sub>2</sub>). Therefore, the loading amount of Ru NPs increased with the increasing calcination temperature (Table S1) due to the increased weight ratio between Ru and C/TiO<sub>2</sub> for the samples prepared at higher temperatures.

We anticipate that the synthesized materials could serve as excellent catalysts for selective hydrogenation reactions, owing to their ultra-small and uniform particle sizes of Ru NPs, low

crystallinity (i.e., poorly ordered structure) and mesoporous structures. In recent years, upgrading of the biomass derived compounds to value added chemicals and/or fuel products in an effective and selective manner is important to fully exploit the chemical potential of these valuable resources.<sup>19-21</sup> However, due to the presence of diverse functionalities in many platform molecules derived from biomass (e.g., furfural, 5-hydroxymethylfurfural), hydrotreatment of these substrates generally results in a mixture of products and the reaction pathways are complicated.<sup>22-24</sup>

Selective hydrotreatment of furfural to value-added products over various metal NPs such as Ni,<sup>25</sup> Ru,<sup>26</sup> Cu<sup>27</sup> and bimetallic catalysts<sup>28</sup> have been extensively studied. Herein, the catalytic properties of the synthesized Ru@C/TiO<sub>2</sub> catalysts for selective hydrogenation of furfural were studied. For the Ru@C/TiO<sub>2</sub>-500 catalyst, the conversion of furfural gradually increases with reaction time and reaches around 100% after 4 h at 80 °C (Figure 4A). The yield of tetrahydrofurfuryl alcohol (THFA) reaches around 100% after 5 h reaction at 80 °C and furfural alcohol (FA) was detected as the intermediate product. For comparison, the reaction could not proceed without Ru@C/TiO<sub>2</sub>. By adjusting the reaction conditions, the yield of THFA (ca. 98%) could be achieved with nearly 100% furfural conversion at 120 °C for 1 h (Figure 4B). Further increasing the reaction temperature to 140 °C leads to ring opening reactions of THFA and trace amounts of 1, 2-pentanediol was generated as a side product (Figure 4B).

**Table 1.** Hydrogenation of furfural over Ru@C/TiO<sub>2</sub>.<sup>[a]</sup>

Entry	Catalyst	Temperature/°C	Time/h	Conversion/%	Y (S) of FA <sup>[b]</sup> /%	Y (S) of THFA <sup>[c]</sup> /%	TOF <sup>[d]</sup>	CB <sup>[e]</sup> /%
1	Ru@C/TiO <sub>2</sub> -500	40	1	16	15 (94)	0	44	94
2	Ru@C/TiO <sub>2</sub> -500	40	4	53	51 (96)	0	37	96
3	Ru@C/TiO <sub>2</sub> -500	40	7	>99	96 (96)	3 (3)	40	99
4	Ru@C/TiO <sub>2</sub> -400	80	5	>99	0	98 (98)	72	98
5	Ru@C/TiO <sub>2</sub> -400	40	7	>99	97 (97)	4 (4)	51	101
6	Ru@C/TiO <sub>2</sub> -600	80	5	>99	0	99 (99)	50	99
7	Ru@C/TiO <sub>2</sub> -600	40	7	>99	85 (85)	12 (12)	31	97
8	Ru@C/TiO <sub>2</sub> -700	80	5	>99	0	98 (98)	49	98
9	Ru@C/TiO <sub>2</sub> -700	40	7	>99	80 (80)	16 (16)	28	96
10 <sup>[f]</sup>	Ru/C (5%)	40	7	92	87 (94)	4 (4)	31	98
11 <sup>[g]</sup>	Ru/TiO <sub>2</sub> , RT, H <sub>2</sub> (0.3 MPa), solvent: octane			8.2	8.2 (100)	0	---	---
12 <sup>[h]</sup>	Ru/C, 165 °C, H <sub>2</sub> (2.5 MPa), solvent: water			100	0	7 (7)	---	---
13 <sup>[h]</sup>	Ru/C, 165 °C, H <sub>2</sub> (2.5 MPa), solvent: 1-butanol			89	20 (23)	6 (7)	---	---
14 <sup>[h]</sup>	Ru/C, 165 °C, H <sub>2</sub> (2.5 MPa), solvent: MTHF <sup>[i]</sup>			91	38 (42)	10 (11)	---	---

[a] Reaction conditions: furfural: 1 mmol; catalyst: 30 mg; 1-butanol: 3 mL; H<sub>2</sub> pressure: 4 MPa. [b] FA: furfural alcohol; Y: Yield; S: selectivity; [c] THFA: tetrahydrofurfuryl alcohol; Y: Yield; S: selectivity; [d] Turnover number (TON)=mol of product per mole of Ru; TOF=TON h<sup>-1</sup>. The TOF was obtained based on the sole product; [e] CB: carbon balance; [f] The amount of Ru/C (5%) was 8 mg; [g] The data was obtained from Ref. 29; [h] The data was obtained from Ref. 30; [i] MTHF: 2-Methyltetrahydrofuran

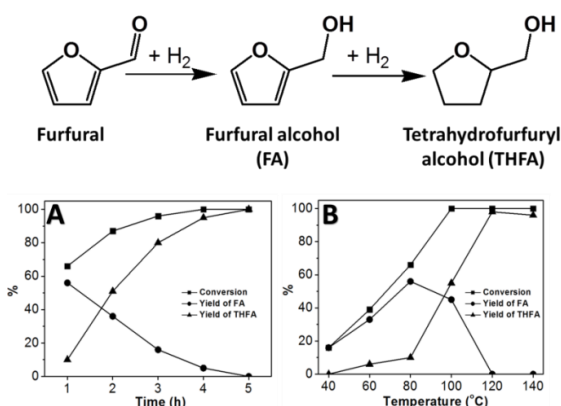


**Figure 4.** Hydrogenation of furfural over Ru@C/TiO<sub>2</sub>-500 under different conditions (furfural: 1 mmol; catalyst: 30 mg; 1-butanol: 3 mL; H<sub>2</sub> pressure: 4 MPa).

Furfural alcohol (FA) is one of the most attractive molecules that could be derived from hydrogenation of furfural. Hence, it is important to achieve selective hydrogenation of the aldehyde group of furfural while leaving the furan ring intact. We noticed that when the reaction was conducted at 40 °C for 1 h with Ru@C/TiO<sub>2</sub>-500, the selectivity of FA could reach ca. 94% at 16% conversion (Table 1, entry 1). Further increasing the reaction time to 7 h, the yield and selectivity of FA could be increased to around 96% (Table 1, entry 2 and 3).

Due to the similar chemical and structural properties of Ru@C/TiO<sub>2</sub>-400 to Ru@C/TiO<sub>2</sub>-500, their catalytic activities are similar. The yield of THFA was ca. 98% with nearly 100% conversion of furfural at 80 °C for 5 h (Table 1, Entry 4) while the yield of FA was ca. 97% at 40 °C for 7 h (Table 1, Entry 5) over Ru@C/TiO<sub>2</sub>-400. For the reactions conducted with Ru@C/TiO<sub>2</sub>-600 and Ru@C/TiO<sub>2</sub>-700, high conversion furfural (> 99%) and selectivity of THFA (> 98%) were achieved at 80 °C for 5 h. However, their selectivities towards FA was lower than those of Ru@C/TiO<sub>2</sub>-400 and Ru@C/TiO<sub>2</sub>-500 at 40 °C for 7 h (Table 1, entry 6-9) From our experimental results, there were no other solid or gaseous products generated from the reaction and the carbon balance of the reaction system was around 100%. Furthermore, it is noteworthy that the Ru@C/TiO<sub>2</sub>-500 catalyst could be reused at least five times without obvious decline of activity under various reaction conditions (Figure 5). Additionally, it was found that the activity of our prepared catalyst (Ru@C/TiO<sub>2</sub>-500) was higher than the commercial Ru/C (Table 1, entry 10) and some reported catalysts (Table 1, entry 11-14).<sup>29-31</sup>

In summary, we have developed a simple and effective method for the synthesis of porous heterogeneous catalysts containing Ru NPs with ultra-small particle sizes (< 2 nm) and narrow size distribution, taking advantage of the coordination effect between naturally occurring polyphenol (TA) and metal ions. These novel and robust catalysts exhibited high activity for selective hydrogenation of furfural and the product could be tuned to either FA or THFA by adjusting the reaction conditions. We envisage that this novel, green and readily applicable

methodology for the preparation of ultra-small noble metal NPs will find a diverse range of applications.

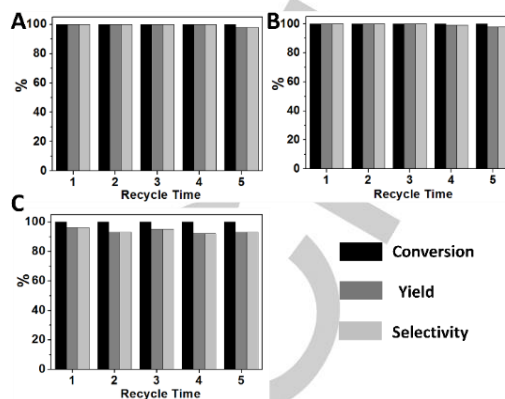


**Figure 5.** Reusability of Ru@C/TiO<sub>2</sub>-500 for catalytic conversion of furfural, (A) at 80 °C for 5 h, yield and selectivity: THFA; (B) at 120 °C for 1 h, yield and selectivity: THFA; (C) at 40 °C for 7 h, yield and selectivity: FA. Other reaction conditions: furfural 1 mmol; catalyst: 30 mg; 1-butanol: 3 mL; H<sub>2</sub> pressure: 4 MPa.

## Acknowledgements

The authors acknowledge the National Natural Science Foundation of China (21603236, 21673249 and 21503238) and the Youth Innovation Promotion Association of CAS (2017043).

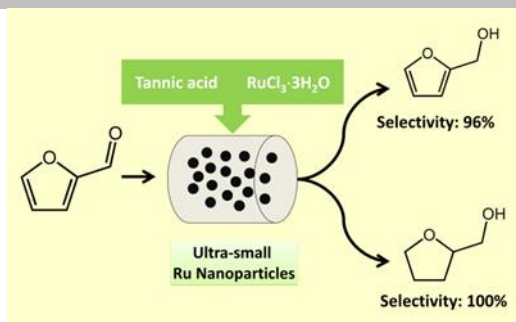
**Keywords:** Natural resources • polyphenols • heterogeneous catalysis • ultra-small metal nanoparticles • furfural hydrogenation

- [1] a) S. Cao, F. Tao, Y. Tang, Y. Li and J. Yu, *Chem. Soc. Rev.* **2016**, *45*, 4747-4765; b) T. Chen and V. O. Rodionov, *ACS Catal.* **2016**, *6*, 4025-4033; c) S. Zhang, L. Nguyen, Y. Zhu, S. Zhan, C.-K. Tsung and F. Tao *Acc. Chem. Res.* **2013**, *46*, 1731-1739.
- [2] M. Turner, V. B. Golovko, O. P. H. Vaughan, P. Abdulkin, A. Berenguer-Murcia, M. S. Tikhov, B. F. G. Johnson and R. M. Lambert, *Nature* **2008**, *454*, 981-983.
- [3] B. Liu, H. Yao, W. Song, L. Jin, I. M. Mosa, J. F. Rusling, S. L. Suib and J. He, *J. Am. Chem. Soc.* **2016**, *138*, 4718-4721.
- [4] a) G.-H. Wang, Z. Cao, D. Gu, N. Pfänder, A.-C. Swertz, B. Spliethoff, H.-J. Bongard, C. Weidenthaler, W. Schmidt, R. Rinaldi and F. Schüth, *Angew. Chem. Int. Ed.* **2016**, *55*, 8850-8855; b) X. Kang, J. Zhang, W. Shang, T. Wu, P. Zhang, B. Han, Z. Wu, G. Mo and X. Xing, *J. Am. Chem. Soc.* **2014**, *136*, 3768-3771; c) Y. Liu, H. Tsunoyama, T. Akita, S. Xie and T. Tsukuda, *ACS Catal.* **2011**, *1*, 2-6.
- [5] R. J. White, R. Luque, V. L. Budarin, J. H. Clark and D. J. Macquarrie, *Chem. Soc. Rev.* **2009**, *38*, 481-494.
- [6] M. Cargnello, C. Chen, B. T. Diroll, V. V. T. Doan-Nguyen, R. J. Gorte and C. B. Murray, *J. Am. Chem. Soc.* **2015**, *137*, 6906-6911.
- [7] a) P. Hu, J. V. Morabito and C.-K. Tsung, *ACS Catal.* **2014**, *4*, 4409-4419; b) C. Wang, L. Wang, J. Zhang, H. Wang, J. P. Lewis and F.-S. Xiao, *J. Am. Chem. Soc.* **2016**, *138*, 7880-7883.
- [8] E. Munch, M. E. Launey, D. H. Alsem, E. Saiz, A. P. Tomsia and R. O. Ritchie, *Science* **2008**, *322*, 1516-1520.
- [9] S. Quideau, D. Deffieux, C. Douat-Casassus and L. Pouységu, *Angew. Chem. Int. Ed.* **2011**, *50*, 586-621.
- [10] T. Sylla, L. Pouységu, G. Da Costa, D. Deffieux, J.-P. Monti and S. Quideau, *Angew. Chem. Int. Ed.* **2015**, *54*, 8217-8221.

- [11] J. H. Park, K. Kim, J. Lee, J. Y. Choi, D. Hong, S. H. Yang, F. Caruso, Y. Lee and I. S. Choi, *Angew. Chem. Int. Ed.* **2014**, *53*, 12420-12425.
- [12] a) J. Wei, Y. Liang, Y. Hu, B. Kong, G. P. Simon, J. Zhang, S. P. Jiang and H. Wang, *Angew. Chem. Int. Ed.* **2016**, *55*, 1355-1359; b) J. Wei, Y. Liang, Y. Hu, B. Kong, J. Zhang, Q. Gu, Y. Tong, X. Wang, S. P. Jiang and H. Wang, *Angew. Chem. Int. Ed.* **2016**, *55*, 12470-12474.
- [13] J. Song, B. Zhou, H. Zhou, L. Wu, Q. Meng, Z. Liu and B. Han, *Angew. Chem. Int. Ed.* **2015**, *54*, 9399-9403.
- [14] T. S. Sileika, D. G. Barrett, R. Zhang, K. H. A. Lau and P. B. Messersmith, *Angew. Chem. Int. Ed.* **2013**, *52*, 10766-10770.
- [15] J. Guo, Y. Ping, H. Ejima, K. Alt, M. Meissner, J. J. Richardson, Y. Yan, K. Peter, D. von Elverfeldt, C. E. Hagemeyer and F. Caruso, *Angew. Chem. Int. Ed.* **2014**, *53*, 5546-5551.
- [16] W. Xu, X. Liu, J. Ren, P. Zhang, Y. Wang, Y. Guo, Y. Guo and G. Lu, *Catal. Commun.* **2010**, *11*, 721-726.
- [17] a) L. H. Wee, S. R. Bajpe, N. Janssens, I. Hermans, K. Houthoofd, C. E. A. Kirschhock and J. A. Martens, *Chem. Commun.*, **2010**, *46*, 8186-8188; b) J. Hafizovic, M. Bjørgen, U. Olsbye, P. D. C. Dietzel, S. Bordiga, C. Prestipino, C. Lamberti and K. P. Lillerud, *J. Am. Chem. Soc.*, **2007**, *129*, 3612-3620.
- [18] Z. Sun, Z. Liu, B. Han, S. Miao, Z. Miao and G. An, *J. Colloid Interface Sci.* **2006**, *304*, 323-328.
- [19] a) M. Besson, P. Gallezot and C. Pinel, *Chem. Rev.* **2014**, *114*, 1827-1870; b) P. Gallezot, *Chem. Soc. Rev.* **2012**, *41*, 1538-1558.
- [20] a) J. Julis and W. Leitner, *Angew. Chem. Int. Ed.* **2012**, *51*, 8615-8619; b) D. M. Alonso, S. G. Wettstein and J. A. Dumesic, *Chem. Soc. Rev.* **2012**, *41*, 8075-8098; c) C.-H. Zhou, X. Xia, C.-X. Lin, D.-S. Tong and J. Beltramini, *Chem. Soc. Rev.* **2011**, *40*, 5588-5617.
- [21] Z. Zhang, J. Song and B. Han, *Chem. Rev.* **2016**, DOI: 10.1021/acs.chemrev.6b00457.
- [22] a) R. Mariscal, P. Maireles-Torres, M. Ojeda, I. Sadaba and M. Lopez Granados, *Energy Environ. Sci.* **2016**, *9*, 1144-1189; b) A. J. Garcia-Olmo, A. Yopez, A. M. Balu, A. A. Romero, Y. Li and R. Luque, *Catal. Sci. Technol.* **2016**, *6*, 4705-4711.
- [23] R. Fang, H. Liu, R. Luque and Y. Li, *Green Chem.* **2015**, *17*, 4183-4188.
- [24] a) J. Jae, W. Zheng, A. M. Karim, W. Guo, R. F. Lobo and D. G. Vlachos, *ChemCatChem*, **2014**, *6*, 848-856; b) L. Yu, L. He, J. Chen, J. Zheng, L. Ye, H. Lin and Y. Yuan, *ChemCatChem*, **2015**, *7*, 1701-1707.
- [25] a) Y. Nakagawa, H. Nakazawa, H. Watanabe and K. Tomishige, *ChemCatChem*, **2012**, *4*, 1791-1797; b) T. V. Kotbagi, H. R. Gurav, A. S. Nagpure, S. V. Chilukuri and M. G. Bakker, *RSC Adv.*, **2016**, *6*, 67662-67668.
- [26] a) J. Chen, F. Lu, J. Zhang, W. Yu, F. Wang, J. Gao and J. Xu, *ChemCatChem*, **2013**, *5*, 2822-2826; b) Z. Gao, L. Yang, G. Fan and F. Li, *ChemCatChem*, **2016**, *8*, 3769-3779; c) A. D. Dwivedi, K. Gupta, D. Tyagi, R. K. Rai, S. M. Mobin and S. K. Singh, *ChemCatChem*, **2015**, *7*, 4050-4058; d) P. Panagiotopoulou, N. Martin and D. G. Vlachos, *ChemSusChem*, **2015**, *8*, 2046-2054.
- [27] H. Sheng and R. F. Lobo, *ChemCatChem*, **2016**, *8*, 3402-3408.
- [28] a) S. T. Thompson and H. H. Lamb, *ACS Catal.*, **2016**, *6*, 7438-7447; b) X. Chang, A.-F. Liu, B. Cai, J.-Y. Luo, H. Pan and Y.-B. Huang, *ChemSusChem*, **2016**, *9*, 3330-3337.
- [29] O. F. Aldosari, S. Iqbal, P. J. Miedziak, G. L. Brett, D. R. Jones, X. Liu, J. K. Edwards, D. J. Morgan, D. K. Knight and G. J. Hutchings, *Catal. Sci. Technol.* **2016**, *6*, 234-242.
- [30] V. V. Ordonsky, J. C. Schouten, J. van der Schaaf and T. A. Nijhuis, *Appl. Catal. A: Gen.*, **2013**, *451*, 6-13.
- [31] K. Yan, G. Wu, T. Lafleur and C. Jarvis, *Renew. Sust. Energ. Rev.*, **2014**, *38*, 663-676.

## Entry for the Table of Contents

Mesoporous heterogeneous catalysts containing ultra-small Ru NPs were synthesized using natural precursor and are highly efficient for selective furfural hydrogenation.



Zhanrong Zhang, Jinliang Song\*,  
Zhiwei Jiang, Qinglei Meng, Pei  
Zhang and Buxing Han\*

Page No. – Page No.

Direct Synthesis of Ultra-small  
Ruthenium Nanoparticles on  
Porous Supports Using Natural  
Sources for Highly Efficient and  
Selective Furfural  
Hydrogenation